Effect of gasification agent on the performance of solid oxide fuel cell and biomass gasification systems

Colpan, C. Ozgur; Hamdullahpur, Feridun; Dincer, Ibrahim; Yoo, Yeong

Publisher's version / Version de l'éditeur:

Proceedings of International Conference on Hydrogen Production, 2009, pp. 322-334, 2009

NRC Publications Record / Notice d'Archives des publications de CNRC:
https://nrc-publications.canada.ca/eng/view/object/?id=f909eeeb-aa5a-49c9-8f1c-7be159174d78
https://publications-cnrc.canada.ca/fra/voir/objet/?id=f909eeeb-aa5a-49c9-8f1c-7be159174d78

EFFECT OF GASIFICATION AGENT ON THE PERFORMANCE OF SOLID OXIDE FUEL CELL AND BIOMASS GASIFICATION SYSTEMS

C. Ozgur Colpan[1], Feridun Hamdullahpur[2], Ibrahim Dincer[3] and Yeong Yoo[4]
[1,2] Mechanical and Aerospace Engineering Department, Carleton University
1125 Colonel By Drive, Ottawa, Ontario, Canada K1S 5B6
[3]Faculty of Engineering and Applied Science, University of Ontario Institute of Technology, 2000 Simcoe Street North, Oshawa, Ontario, Canada L1H 7L7
[4]National Research Council of Canada, Institute for Chemical Process and Environmental Technology, Ottawa, Ontario, Canada, K1A 0R6

ABSTRACT
In this study, an integrated SOFC and biomass gasification system is modeled. For this purpose, energy and exergy analyses are applied to the control volumes enclosing the components of the system. However, SOFC is modeled using a transient heat transfer model developed by the authors in a previous study. Effect of gasification agent, i.e. air, enriched oxygen and steam, on the performance of the overall system is studied. The results show that steam gasification case yields the highest electrical efficiency, power-to-heat ratio and exergetic efficiency, but the lowest fuel utilization efficiency. For this case, it is found that electrical, fuel utilization and exergetic efficiencies are 41.8%, 50.8% and 39.1%, respectively, and the power-to-heat ratio is 4.649.

INTRODUCTION
Biomass has increased its importance due to the fact that it can be utilized as a potential fuel source in advanced energy systems. Also, systems based on biomass fuel are considered to contribute to the sustainable development in industrialized and developing countries. In this regard, researchers tend to find solutions to obtain efficient and economical heat and electricity generation from biomass fuel.

There are various types of biomass, such as wood, landfill gas, crops, alcohol fuels, and municipal solid wastes. Biomass has a share of 10.7% in the total global primary energy use and 1.1% in the world electricity production (Goldemberg and Johansson, 2004). It is expected that the biomass share of electricity output will increase to a point between 2% and 5.1% in 2050 according to the different scenarios (International Energy Agency, 2007). Conventionally, biomass is converted to electricity is by combustion of the feedstock to raise steam that is used to drive the steam turbine. Other technologies include externally fired gas turbines, integrated gasification combined cycles and fuel cells.

Among the different types of fuel cells, MCFC and SOFC are considered the most promising ones for biomass fueled fuel cells due to their high operating temperature level, flexibility to different fuel and greater tolerance to contaminants. According to the biomass conversion method, some of the other fuel cell types may also be useful. For example, landfill gas and digester gas may be used with PAFC today and their usage with this kind of fuel cell has been successfully demonstrated (Xenergy, 2002). Additionally, the suitability of biogas as a fuel for PEMFC has been experimentally confirmed (Schmersahl and Scholz, 2005).

Biomass fuelled integrated SOFC system is one of the key energy technologies of the future since it combines the merits of renewable energy sources and hydrogen energy systems. There has been an increasing interest in converting biomass to a product gas by various thermochemical and biochemical methods for using it as a fuel in SOFCs. These methods include gasification, anaerobic digestion, fast pyrolysis and fermentation. The product gas obtained from these conversions contains contaminants such as tars, hydrogen sulfide, alkali compounds, etc., which should be cleaned up according to the tolerance level of the SOFC to the contaminants. The cleaned gas exiting the gas-cleanup system should be reformed to hydrogen and carbon monoxide to be used in the electrochemical reaction; which might be inside or outside the stack.

Panopoulos et al. (2006[1]) investigated the integration of a SOFC with a novel allothermal biomass steam gasification process. They calculated the electrical efficiency of the system as 36% and exergetic efficiency as 32% (Panopoulos et al., 2006[2]). Cordiner et al. (2007) studied the integration of a downdraft gasifier with a SOFC in which woody material is used as the fuel. Electrical efficiency of the system is calculated as 45.8%. In the paper by Athanasiou et al. (2007), integrated SOFC/steam turbine/gasifier system was studied in terms of thermodynamics. The electrical efficiency of the system is found to be 43.3%. The comparison of cold gas cleanup and hot gas cleanup systems to be used in biomass gasification/SOFC system is done by Omosun et al. (2004). They chose co-current fixed bed gasifier for cold gas cleanup and fluidized bed gasifier for hot gas cleanup. After taking into account thermodynamic and economical considerations, they concluded that hot gas cleanup should be preferred.

The objective of this study is to develop a thermodynamic model for integrated SOFC and biomass gasification systems. For this purpose, thermodynamic models for the components of the system such as gasifier, afterburner, blower, etc., are developed. For the SOFC, a pre-developed transient heat transfer model is used. Effect of gasification agent on the performance of the system is studied. Performance assessment parameters are taken as: Electrical efficiency, fuel utilization efficiency, power-to-heat ratio, and exergetic efficiency. Additionally, exergy analysis is applied to the control volumes to calculate the exergy destructions and losses within the system.

DESCRIPTION OF THE SYSTEM

A schematic of the integrated biomass gasification and SOFC system is shown in Figure 1. In this system, biomass enters the dryer to bring its moisture content to a level acceptable by the gasifier. According to the gasification agent, one of the following substances enters the gasifier: air, enriched oxygen or steam. The gas produced by gasification, which is called syngas, has high amounts of tar, sulphur and other contaminants which may cause degradation in SOFCs. Due to this fact, a gas cleanup should be used to clean the syngas according to the SOFC impurity levels. In this study, a hot gas cleanup is chosen. The cleaned syngas enters the SOFC, where electricity is produced. To prevent the carbon deposition, anode recirculation ratio is adjusted. The depleted fuel and air streams enter the afterburner to burn the unused fuel and increase the temperature of the depleted gas streams leaving the SOFC. The burned gas is used to increase the temperature of air supplied by the blower to the SOFC temperature level. The same gas stream supplies heat to the steam generator, and then to the gasifier in the case of steam gasification. Finally, the same gas stream supplies heat to the dryer and it is emitted to the atmosphere.

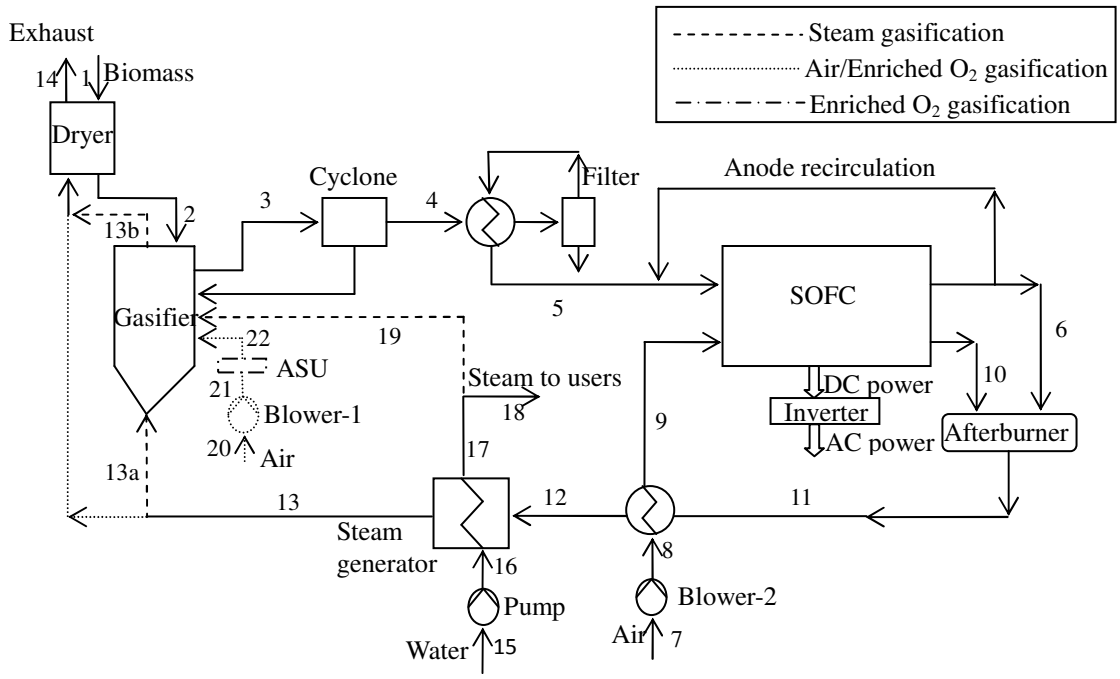

Fig. 1: Schematic of the integrated biomass gasification and SOFC system

A number is given to each state. In Figure 1, 20 and 22 are valid for both the air and oxygen enriched gasification cases. State 21 is only valid for enriched oxygen gasification case. State 13a, 13b, and 19 are only valid for the steam case. The differences in configurations are represented with different dashed lines, which are labelled on Figure 1.

MODELING

The main approach in the modeling is as follows: The syngas composition is first calculated using the gasifier model. Then, using this composition and other SOFC operating parameters, the 2-D transient SOFC code that is developed by the authors (Colpan et al., 2008) is run. This code gives us the molar flow rate at the inlet and exit of gas channels, power output, and temperature at the exit of gas channels for a single cell. According to the power requirement of the SOFC, the number of SOFC stacks that must be used in this system is found. Then, using the output data from the gasifier and SOFC models, the molar flow rate of dry biomass is calculated. Using this molar flow rate and applying energy balances to the remaining components, the enthalpy flow rate of all states, work input to the blowers and pump, if applicable, are calculated.

The main assumptions in this model are as follows:

- The system operates at steady state

- Kinetic and potential energy effects are ignored.
- Ideal gas principles apply for the gases.
- The syngas produced by the gasifier is at chemical equilibrium
- The impurities such as tar, sulphur, ammonia are not considered in the calculations.
- Heat losses from the components are neglected.
- High temperature blower for anode recirculation is not shown in the figure and its work input is neglected.
- All of the steam export returns as condensate.
- Complete combustion occurs in the combustor.

As an example, the modeling equations for the steam gasification case are given below.

The chemical equation in the dryer may be shown as follows

$$C_xH_yO_z + m_1H_2O_{(l)} \rightarrow C_xH_yO_z + m_2H_2O_{(l)} + (m_1 - m_2)H_2O_{(v)} \quad (1)$$

The gasification reaction may be given as

$$C_xH_yO_z + m_2H_2O_{(l)} + (m_1 - m_2)H_2O_{(v)} + \lambda H_2O_{(v)} + q_{added} \rightarrow \alpha_1 CH_4 + \alpha_2 H_2 + \alpha_3 CO + \alpha_4 CO_2 + \alpha_5 H_2O \quad (2)$$

In Eq. (2), we fix λ, hence there are six unknowns, which are: α_1, α_2, α_3, α_4, α_5, and q_{added}. We need six equations to find these unknowns. These equations are 3 atom balances, Eqs. (3)-(5),chemical equilibrium relations for water-gas shift reaction and methanation reaction, Eqs. (6) and (7), and the energy balance around the control volume enclosing the gasifier, Eq. (8).

$$x = \alpha_1 + \alpha_3 + \alpha_4 \quad (3)$$

$$y + 2m_1 + 2\lambda = 4\alpha_1 + 2\alpha_2 + 2\alpha_5 \quad (4)$$

$$z + m_1 + \lambda = \alpha_3 + 2\alpha_4 + \alpha_5 \quad (5)$$

$$K_{wgs} = \exp\left[-\Delta\bar{g}^{\circ}_{wgs} / RT\right] = \frac{x_{CO_2} \cdot x_{H_2}}{x_{CO} \cdot x_{H_2O}} \quad (6)$$

$$K_m = \exp\left[-\Delta\bar{g}^{\circ}_{m} / RT\right] = \frac{x_{CH_4}}{x_{H_2}^{\,2}} \cdot \left(\frac{P}{P_o}\right)^{-1} \quad (7)$$

$$\bar{h}^{\circ}_{2,C_xH_yO_z} + m_2 \cdot \bar{h}^{\circ}_{2,H_2O(l)} + (m_1 - m_2) \cdot \bar{h}^{\circ}_{2,H_2O(v)} + \lambda \cdot \bar{h}^{\circ}_{19,H_2O(v)} + q_{added} = \alpha_1 \bar{h}^{\circ}_{3,CH_4} + \alpha_2 \bar{h}^{\circ}_{3,H_2} + \alpha_3 \bar{h}^{\circ}_{3,CO} + \alpha_4 \bar{h}^{\circ}_{3,CO_2} + \alpha_5 \bar{h}^{\circ}_{3,H_2O} \quad (8)$$

The transient heat transfer modeling equations for SOFC are given in the paper by Colpan et al. (2008). The modeling approach and the main features of the model are as follows:

- A control volume around the repeat element of a planar, co-flow, DIR-SOFC is taken.
- Solid structure is modeled in 2-D, whereas gas channels are modeled in 1-D.
- Cell voltage, Reynolds number at the fuel channel inlet, and excess air coefficient are input parameters. Current density, temperature, and molar gas composition distributions, fuel utilization, power output and electrical efficiency of the cell are output parameters.
- Six gas species, CH_4, H_2, CO, CO_2, H_2O and N_2 at the fuel channel inlet and two gas species O_2 and N_2 at the air channel inlet are considered.
- Fully developed laminar flow conditions are assumed in channels.
- Convection in the rectangular ducts and surface-to-surface radiation effects, conduction heat transfer at the section where the interconnects are in contact with PEN structure, ohmic, activation and concentration polarizations are considered.
- The code is written in MatLAB.
- The model is validated with the results from IEA Benchmark Test (Achenbach, 1996).

Using the SOFC model discussed above, the code developed for the transient heat transfer model is run several times to obtain a desired fuel utilization for a given cell geometry, cell voltage, Reynolds number and

excess air coefficient. Using this code, output for a single cell is obtained. For this output, number of stacks needed for the system can be calculated as follows

$$n_{stack} = \frac{\dot{W}_{req,SOFC}}{w_{SOFC} \cdot n_{cps}} \tag{9}$$

We should take the closest integer higher than the value obtained by Eq. (9). Then, power output of SOFC, molar flow rate of gas species at the fuel and air channels inlets and exits can be calculated for the total amount of stacks calculated.

At this point, we can calculate the molar flow rate of dry biomass entering the system using Eq. (10).

$$\dot{n}_{C_xH_yO_z} = \frac{\sum_{k=1}^{5} \dot{n}_{k,fc.inlet}}{\alpha_1 + \alpha_2 + \alpha_3 + \alpha_4 + \alpha_5} \tag{10}$$

If we consider complete combustion in the afterburner, the chemical reaction occurring in the afterburner may be given as,

$$\dot{n}_{6,CH_4} CH_4 + \dot{n}_{6,H_2} H_2 + \dot{n}_{6,CO} CO + \dot{n}_{6,CO_2} CO_2 + \dot{n}_{6,H_2O} H_2O + \dot{n}_{6,N_2} N_2 + \dot{n}_{10,O_2} O_2 + \dot{n}_{10,N_2} N_2 \rightarrow \dot{n}_{11,CO_2} CO_2 + \dot{n}_{11,H_2O} H_2O + \dot{n}_{11,O_2} O_2 + \dot{n}_{11,N_2} N_2 \tag{11}$$

The molar flow rates of gas species at states 6 and 10 are known from the SOFC model. We can calculate the molar flow rates of gas species at state 11 using the atom balances, Eqs. (12)-(15), and the enthalpy flow rate of this state can be found using an energy balance around the control volume enclosing the afterburner, Eq. (16).

$$\dot{n}_{11,CO_2} = \dot{n}_{6,CH_4} + \dot{n}_{6,CO} + \dot{n}_{6,CO_2} \tag{12}$$

$$\dot{n}_{11,H_2O} = 2 \cdot \dot{n}_{6,CH_4} + \dot{n}_{6,H_2} + \dot{n}_{6,H_2O} \tag{13}$$

$$\dot{n}_{11,O_2} = \dot{n}_{6,CO} / 2 + \dot{n}_{6,CO_2} + \dot{n}_{6,H_2O} / 2 + \dot{n}_{10,O_2} - \dot{n}_{11,CO_2} - \dot{n}_{11,H_2O} / 2 \tag{14}$$

$$\dot{n}_{11,N_2} = \dot{n}_{6,N_2} + \dot{n}_{10,N_2} \tag{15}$$

$$\dot{H}_{11} = \sum_{k=1}^{6} \left(\dot{n}_{6,k} \cdot \bar{h}_{6,k} \right) + \sum_{l=1}^{2} \left(\dot{n}_{10,l} \cdot \bar{h}_{10,l} \right) \tag{16}$$

where k denotes CH_4, H_2, CO, CO_2, H_2O and N_2; whereas l denotes O_2 and N_2.

The specific enthalpy of state 8 may be written as

$$\bar{h}_8 = \bar{h}_7 + \frac{(P_8 - P_7) \cdot M_{air}}{\rho_{air} \cdot \eta_{blower}} \tag{17}$$

Specific work input to blower may be given as

$$\dot{W}_{blower} = \left(\dot{n}_{9,O_2} + \dot{n}_{9,N_2} \right) \cdot \left(\bar{h}_8 - \bar{h}_7 \right) \tag{18}$$

From an energy balance around the control volume enclosing the heat exchanger, enthalpy flow rate of state 12 may be found as follows.

$$\dot{H}_{12} = \dot{H}_{11} + \sum_{l=1}^{2} \left(\dot{n}_{8,l} \cdot \bar{h}_{8,l} \right) - \sum_{l=1}^{2} \left(\dot{n}_{9,l} \cdot \bar{h}_{9,l} \right) \tag{19}$$

From an energy balance around the control volume enclosing the dryer, enthalpy flow rate of state 13b may be found as follows.

$$\dot{H}_{13b} = \sum_{m=1}^{4} \left(\dot{n}_{11,m} \cdot \bar{h}_{14,m} \right) + \dot{n}_{C_xH_yO_z} \cdot \left(\bar{h}_{2,C_xH_yO_z} + m_2 \cdot \bar{h}_{2,H_2O(l)} + (m_1 - m_2) \cdot \bar{h}_{2,H_2O(v)} - \bar{h}_{1,C_xH_yO_z} - m_1 \cdot \bar{h}_{1,H_2O(l)} \right) \tag{20}$$

where m denotes CO_2, H_2O, O_2 and N_2.

The specific enthalpy for state 16 may be written as

$$\bar{h}_{16} = \bar{h}_{15} + \frac{v_{15} \cdot (P_{16} - P_{15}) \cdot M_{H_2O}}{\eta_{pump}} \quad (21)$$

At this point, we can calculate the total heat added to the gasifier as follows

$$\dot{Q}_{added} = q_{added} \cdot \dot{n}_{C_xH_yO_z} \quad (22)$$

Enthalpy flow rate of state 13a can be calculated as follows

$$\dot{H}_{13a} = \dot{H}_{13b} + \dot{Q}_{added} \quad (23)$$

From an energy balance around the control volume enclosing the steam generator, the molar flow rate of steam generated may be found.

$$\dot{n}_{17} = \frac{\dot{H}_{12} - \dot{H}_{13a}}{\bar{h}_{17} - \bar{h}_{16}} \quad (24)$$

Work input to pump may be given as

$$\dot{W}_{pump} = \dot{n}_{17} \cdot (\bar{h}_{16} - \bar{h}_{15}) \quad (25)$$

Change of enthalpy flow rate of the process may be shown as

$$\Delta\dot{H}_{process} = (\dot{n}_{17} - \dot{n}_{C_xH_yO_z} \cdot \lambda) \cdot (\bar{h}_{18} - \bar{h}_{15}) \quad (26)$$

Net electrical power output of the system may be given as

$$\dot{W}_{net} = n_{stack} \cdot n_{cps} \cdot w_{SOFC} \cdot \eta_{inv} - \dot{W}_{blower} - \dot{W}_{pump} \quad (27)$$

Electrical efficiency, fuel utilization efficiency, and power-to-heat ratio may be calculated using Eqs. (28)-(30), respectively.

$$\eta_{el} = \frac{\dot{W}_{net}}{\dot{n}_{C_xH_yO_z} \cdot (LHV + m_1 \cdot \bar{h}_{fg})} \quad (28)$$

$$FUE = \frac{\dot{W}_{net} + \Delta\dot{H}_{process}}{\dot{n}_{C_xH_yO_z} \cdot (LHV + m_1 \cdot \bar{h}_{fg})} \quad (29)$$

$$PHR = \frac{\dot{W}_{net}}{\Delta\dot{H}_{process}} \quad (30)$$

After energy analysis is completed, exergy analysis is conducted. In this analysis, exergy balance which is derived by combining first and second laws of thermodynamics (Bejan et al., 1996), is applied to the control volumes applying the components. The steady state form of control volume exergy balance may be given as

$$0 = \sum_j \left(1 - \frac{T_o}{T_j}\right) \cdot \dot{Q}_j - \dot{W}_{cv} + \sum_i \dot{n}_i \cdot ex_i - \sum_e \dot{n}_e \cdot ex_e - \dot{E}x_D \quad (31)$$

In Eq. (31), *ex* represents the specific molar exergy. The components of specific exergy are discussed below. $\dot{E}x_D$ represents the exergy destruction in the control volume. Exergy losses are included in the fourth term of Eq. (31).

If we neglect the magnetic, electrical, nuclear, kinetic and potential effects, there are mainly two types of exergy: pyhsical and chemical. The first one measures the amount of work when the system comes into thermal ($T = T_o$) and mechanical ($P = P_o$) equilibrium. This condition is called as restricted dead state. Chemical exergy gives the amount of work when the system is brought from restricted dead state to dead state. As discussed earlier, at dead state, in addition to the thermal and mechanical equilibrium, the system is also at chemical equilibrium ($\mu=\mu_o$).

The physical flow exergy for simple, compressible pure substances is given as

$$ex^{PH} = (h - h_o) - T_o(s - s_o) \quad (32)$$

Chemical exergy may be found using the tables available in the literature (Szargut et al., 1988; Szargut et al., 2005). For an ideal gas mixture, Eqn. (33) can be used to calculate the specific molar chemical exergy of the mixture.

$$ex^{CH} = \sum x_k \cdot \bar{e}x_k^{CH} + \bar{R} \cdot T_o \cdot \sum x_k \cdot \ln x_k \quad (33)$$

The exergy destruction rate in a component may be compared to the exergy rate of the fuel provided to the overall system as follows;

$$y_D = \frac{\dot{E}x_D}{\dot{E}x_F} \quad (34)$$

The exergy destruction rate of a component may be compared to the total exergy destruction rate within the system giving the ratio.

$$y_D^* = \frac{\dot{E}x_D}{\dot{E}x_{D,tot}} \quad (35)$$

The exergy loss ratio is defined similarly by comparing the exergy loss rate to the exergy rate of the fuel provided to the overall system.

$$y_L = \frac{\dot{E}x_L}{\dot{E}x_F} \quad (36)$$

In defining the exergetic efficiency, it is necessary to identify both a product and a fuel for the thermodynamic system being analyzed. The product represents the desired output produced by the system. The fuel represents the resources expended to generate the product. Exergetic efficiency of a component or system may be given as

$$\varepsilon = \frac{\dot{E}_P}{\dot{E}_F} = 1 - \frac{\dot{E}_D + \dot{E}_L}{\dot{E}_F} \quad (37)$$

Exergetic efficiency of the system can also be defined in terms of exergy destruction ratio and exergy loss ratio.

$$\varepsilon = 1 - \sum y_D - \sum y_L \quad (38)$$

Exergetic efficiency of the system may be defined as

$$\varepsilon = \frac{\dot{W}_{net} + \Delta\dot{E}x_{process}}{\dot{E}x_{ch,C_xH_yO_z} + \dot{n}_{15} \cdot \bar{e}_{ch,H_2O(l)}} \quad (39)$$

$\dot{E}x_{ch,C_xH_yO_z}$ can be found using the correlation given by Szargut (2005). The correlation is modified for this study as follows:

$$\dot{E}x_{ch,C_xH_yO_z} = \beta \cdot \left| \dot{n}_{C_xH_yO_z} \cdot \left(LHV + m_1 \cdot \bar{h}_{fg} \right) \right| \quad (40)$$

where β is defined for solid C,H,O,N compounds (for O/C<2) as Szargut (2005).:

$$\beta = \frac{1.044 + 0.016 \cdot H/C - 0.3493 \cdot O/C \cdot (1 + 0.0531 \cdot H/C) + 0.0493 \cdot N/C}{1 - 0.4124 \cdot O/C} \quad (41)$$

Change of exergetic rate of process may be given as

$$\Delta\dot{E}x_{process} = \left(\dot{n}_{17} - \dot{n}_{C_xH_yO_z} \cdot \lambda \right) \cdot \left(ex_{18} - ex_{15} \right) \quad (42)$$

More information on exergy and its applications can be found in the book by Dincer and Rosen (2005).

RESULTS AND DISCUSSION

The input data used in this study is shown in Table 1. Using this data, syngas composition is first calculated and shown in Table 2. As it can be seen from this table, when enriched oxygen is used instead of air, molar ratio of all species except nitrogen increases due to sending less amount of nitrogen to the gasifier. In the case of using steam as gasification agent, the molar ratios of gases that are used as fuel in SOFC, i.e. CH_4, H_2 and CO are

higher than the cases when we use air or enriched oxygen; however the molar ratio of H_2O is lower than the other cases according to chemical equilibrium calculations.

Table 1: Input data

Environmental temperature	25 ℃
Fuel	
Type of biomass	Wood
Ultimate analysis of biomass [%wt dry basis]	50% C, 6% H, 44% O
Moisture content in biomass [%wt]	40%
Gasifier	
Moisture content in biomass entering gasifier [%wt]	20%
Temperature of syngas exiting gasifier	900 ℃
Molar ratio of steam entering to gasifier to drybiomass	0.1
Molar composition of enriched oxygen	0.35 O_2, 0.65 N_2
SOFC	
Power requirement of SOFC	10 kW
Number of cells per stack	50
Temperature of syngas entering SOFC	850 ℃
Temperature of air entering SOFC	850 ℃
Pressure of the cell	1 atm
Cell voltage	0.65
Excess air coefficient	7
Active cell area	10x10 cm^2
Number of repeat elements per single cell	18
Flow configuration	Co-flow
Manufacturing type	Electrolyte-supported
Thickness of air channel	0.1 cm
Thickness of fuel channel	0.1 cm
Thickness of interconnect	0.3 cm
Thickness of anode	0.005 cm
Thickness of electrolyte	0.015 cm
Thickness of cathode	0.005 cm
Emissivity of PEN	0.8
Emissivity of interconnect	0.1
Diffusivity of anode	0.91 cm^2/s
Diffusivity of cathode	0.22 cm^2/s
Porosity of anode	0.5
Porosity of cathode	0.5
Turtuosity of anode	4
Turtuosity of cathode	4
Balance of Plant	
Temperature of exhaust gas leaving the system	127 °C
Pressure ratio of blowers	1.18
Isentropic efficiency of blowers	0.53
Pressure ratio of pump	1.2
Isentropic efficiency of pump	0.8
Inverter efficiency	0.95

Table 2: Syngas composition (molar basis)

	x_{CH_4}	x_{H_2}	x_{CO}	x_{CO_2}	x_{H_2O}	x_{N_2}
Case1: Air	0.14%	11.22%	8.16%	12.95%	22.68%	44.84%
Case2: Enriched O_2	0.28%	15.74%	11.40%	16.37%	28.80%	27.41%
Case3: Steam	2.15%	43.37%	27.38%	8.98%	18.12%	0.00%

After finding the syngas composition, transient heat transfer code for the SOFC is used to find the fuel cell related output parameters. First, recirculation ratio is taken as zero and the code is run until a fuel utilization of 0.85 is obtained. At this point, the maximum carbon activity through the channel length is checked. If this value is less than 1 for all the nodes, then there is no carbon deposition problem. If this value is higher than 1 for any nodes, then the calculations should be repeated with higher recirculation ratios until the carbon deposition is

prevented. Figure 2 shows that maximum carbon activity is less than 1 for all the nodes for all cases even if we do not recirculate the depleted fuel.

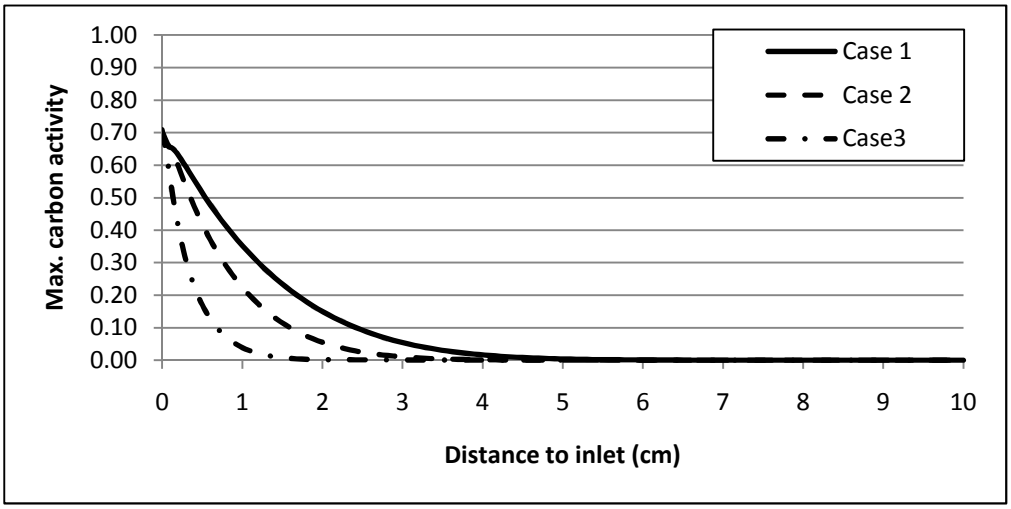

Fig. 2: Change of maximum carbon activity with distance

Figure 3 shows the current density distribution for each case. Since the molar ratio of gas species used as fuel in SOFCs, i.e. CH_4, H_2 and CO, is higher for case 3, higher current densities for each node are obtained for this case compared to other cases. From Table 3, it can be seen that average current densities for cases 1, 2 and 3 are 0.240, 0.246, and 0.343 A/cm^2, respectively. For this table, it can also be interpreted that power density for case-3 is higher than the other cases since we assume the cell voltage as constant in the modeling and average current density is higher for case-3 than other cases. Another interesting result that is found is that 13 stacks are needed for cases 1 and 2, whereas only 9 stacks are needed for case 3. This shows that the purchase equipment cost for case-3 is lower than the other cases.

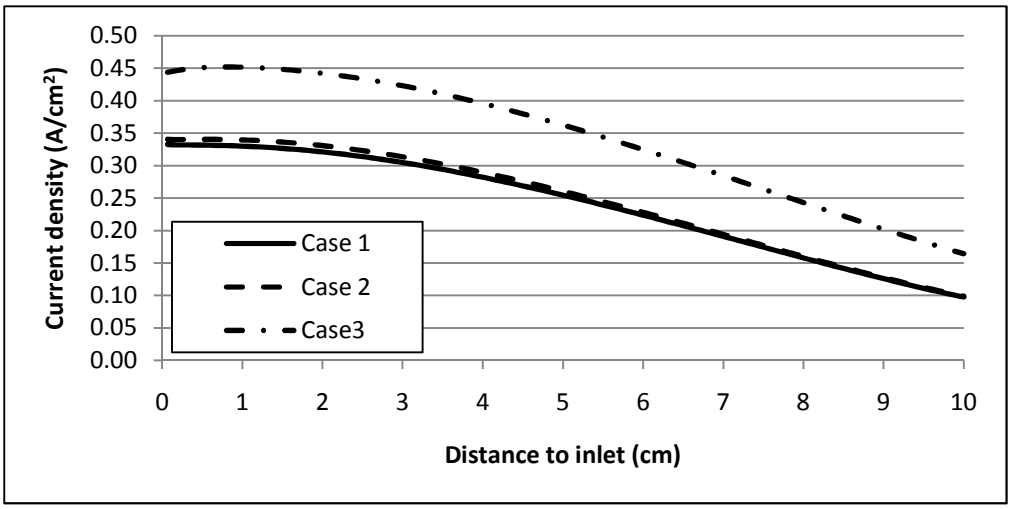

Fig. 3: Change of current density with distance

Table 3: Recirculation ratio, Reynolds Number, average current density, fuel utilization ratio, number of stacks

	r	Re	$i_{c,ave}$ [A/cm^2]	U_F	W_{sofc} [W/cm^2]	n_{stack}
Case1: Air	0	10.0	0.240	0.85	0.156	13
Case2: Enriched O_2	0	6.5	0.246	0.85	0.160	13
Case3: Steam	0	1.5	0.343	0.85	0.223	9

The 2-D temperature profiles of SOFCs are given in Figures 4-6. From these figures, it is seen that temperature gradient in the flow direction is the highest in case 3. Case 2 and case 1 follow it, respectively. It should be noted that the temperature gradients are still less than the maximum allowable value that could cause thermomechanical instability.

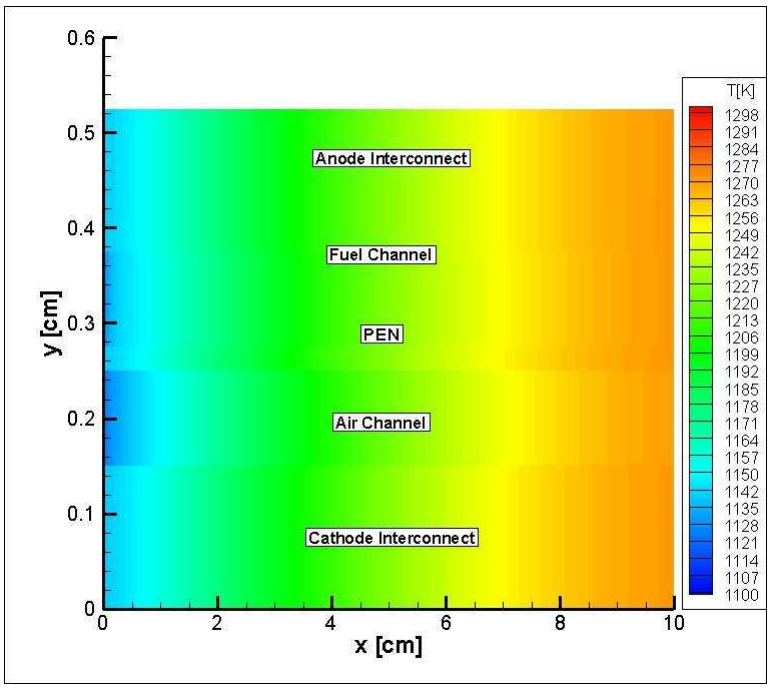

Fig. 4: 2-D temperature profile of SOFC for Case-1 (air gasification)

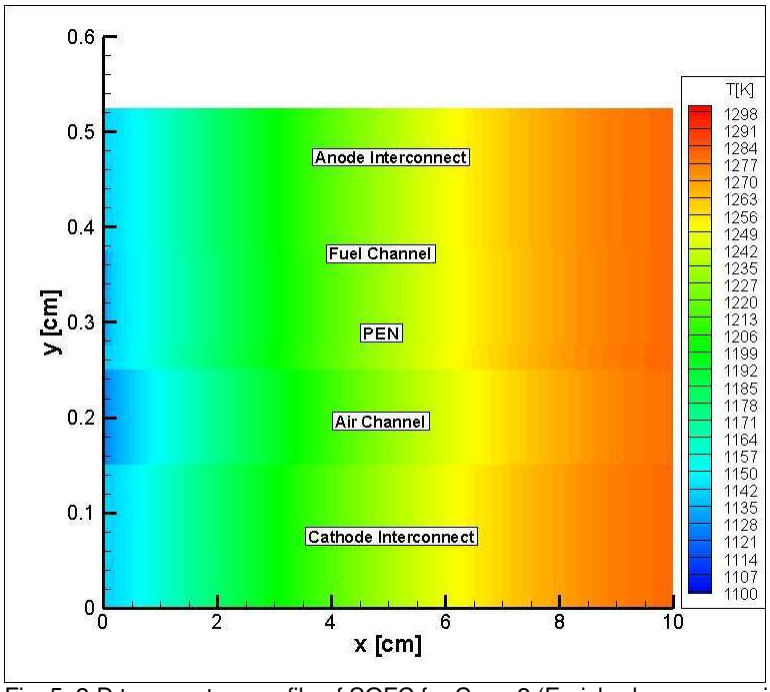

Fig. 5: 2-D temperature profile of SOFC for Case-2 (Enriched oxygen gasification)

The mass flow rates of substances entering the system are given in Table 4. For case 1, we need to feed more biomass to the system, which increases the cost of fuel. Additionally, wood needs to be cut into small pieces before feeding to the system, hence equipment and operation cost for pre-treatment of wood increases for this case. The energy input for the pretreatment operation of wood also increases. It should be noted that pretreatment of wood except drying is not taken into account in the analyses. From Table 4, the mass flow rate of air and water fed to the system, and steam produced and sent to the users can be seen. For case-3, fewer amounts of air and water are fed to the system, which in turn decreases the costs associated with the operation of blowers and pump. However, less amount of steam is produced for this case due to sending high amount of steam to the gasifier for initiating the gasification reactions.

Power input to the auxiliary components, and power output from the system are shown in Table 5. It can be followed from this table that net power output for case-2 is the highest, which is mainly due to higher amount of power obtained for the given number of stacks. Change of enthalpy rate of the process is found to be the highest for case-1 and lowest for case 3. This is because allothermal gasification is used in case-3 and considerable amount of energy is spent in the gasification process, hence less energy remains for producing steam.

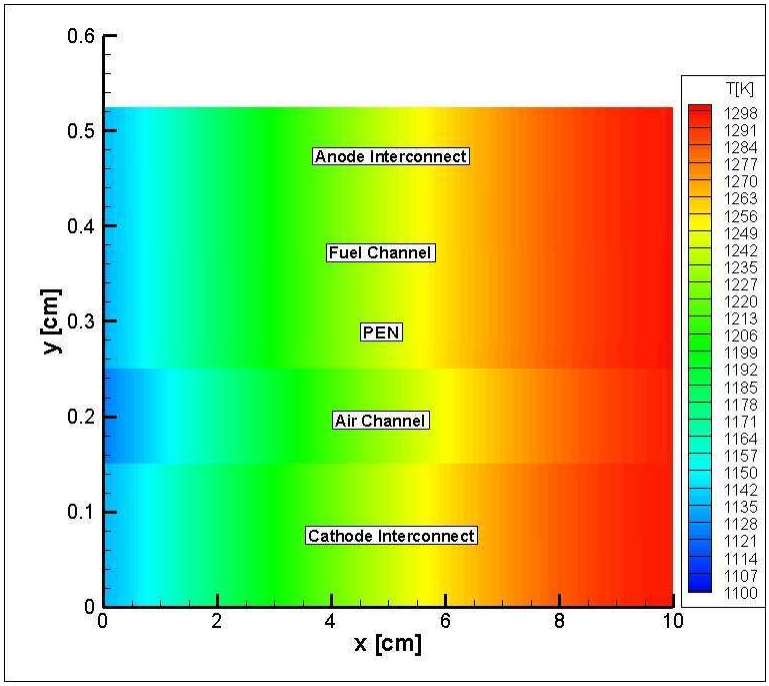

Fig. 6: 2-D temperature profile of SOFC for Case-3 (Steam gasification)

Table 4: Mass flow rate of substances entering the system

	$\dot{m}_{biomass}$ [g/s]	$\dot{m}_{air}$ (B1) [g/s]	$\dot{m}_{air}$ (B2) [g/s]	$\dot{m}_{water}$ [g/s]	$\dot{m}_{steam}$ [g/s]
Case1: Air	4.048	7.796	45.648	7.654	7.654
Case2: Enriched O_2	3.867	6.989	46.841	6.604	6.604
Case3: Steam	1.826	-	45.219	0.7670	0.6847

Table 5: Power demand for auxiliary components, net power and heat output

	$\dot{W}_{SOFC}$ [W]	$\dot{W}_{blower-1}$ [W]	$\dot{W}_{blower-2}$ [W]	$\dot{W}_{pump}$ [W]	$\dot{W}_{net}$ [W]	$\Delta\dot{H}_{process}$ [W]
Case1: Air	10140	227.5	1332.1	0.2	8073.2	19741.3
Case2: Enriched O_2	10384	204.0	1366.9	0.2	8293.7	17032.9
Case3: Steam	10031	-	1319.6	0.02	8210.2	1765.9

Electrical efficiency, fuel utilization efficiency, power-to-heat ratio and exergetic efficiency are chosen as performance assessment parameters in this study. Results are shown in Table 6. It can be seen from this table that case 3 (steam gasification) has the highest electrical efficiency. However, it has also the lowest fuel utilization efficiency since considerable amount of steam is sent to the gasifier and less steam is sent for process heating purposes. In general, producing electricity is more expensive than producing heat. If we compare the power-to-heat ratios, we can see that case 3 is the highest. It may be interpreted from this result that the primary purpose of using the system in case-3 should be producing electricity rather than producing heat. Exergetic efficiency is another way of comparing the overall system performance. In this comparison, the quality of the energy forms together with the quantity of the energy forms is considered. It is seen from Table 6 that exergetic efficiency for case-3 is the highest. When we combine all the results for performance assessment parameters, we can conclude that steam should be selected as the gasification agent to have a better performance in terms of thermodynamics and economics.

Table 6: Performance Assessment Parameters

	η_{el}	*FUE*	*PHR*	ε
Case1: Air	18.5%	63.9%	0.409	30.9%
Case2: Enriched O_2	19.9%	60.9%	0.487	30.7%
Case3: Steam	41.8%	50.8%	4.649	39.1%

We can also use combined air/steam or enriched oxygen/steam gasification agents in the systems. In these cases, molar ratio of oxidant to dry biomass and molar ratio of steam to dry biomass can be altered to get

different results. However, we can expect that the outputs will be between each single case. For example, if we choose enriched oxygen/steam gasification, it is expected that electrical efficiency will be between 19.9% and 41.8% and fuel utilization efficiency will be between 50.8% and 60.9%.

Exergy destructions and losses and their relevant ratios are calculated and the results are shown in Tables 7-9. The results show that, for cases 1 and 2, the largest portion of exergy is destructed in the gasifier. This destruction accounts for 31.02% for case-1 and 30.89% for case-2 of the exergy of the fuel; and 48.60% for case-1 and 48.15% for case-2 of the total exergy destructions. For case-3, the magnitude of exergy destruction for gasifier is much lower than that for cases 1 and 2 because of using allothermal gasification for this case. In this case, the highest exergy is destructed in the heat exchanger, which is 25.65% of the exergy of the fuel and 46.44% of the total exergy destructions. When we compare the exergy losses to environment, it is seen that case-3 has the highest exergy loss, which is equal to the 5.63% of the exergy of the fuel.

Table 7: Exergy destructions in the components and exergy loss to the environment

	Case 1	Case 2	Case 3
Exergy Destructions[W]			
SOFC	664	692	845
Gasifier	15727	14952	837
Afterburner	1622	1800	1490
Dryer	3018	2884	1336
Gas cleanup	678	507	164
Heat exchanger	6421	6453	5834
Blower-1	217	195	-
Blower-2	1272	1305	1260
ASU	-	4	-
Steam generator	2235	1740	295
Water pump	0	0	0
Inverter	507	519	502
Exergy loss [W]	2676	2489	1281

Table 8: Exergy destruction ratios

	Case 1		Case 2		Case 3	
	y_D [%]	y_D^* [%]	y_D [%]	y_D^* [%]	y_D [%]	y_D^* [%]
SOFC	1.31	2.05	1.43	2.23	3.71	6.72
Gasifier	31.02	48.60	30.89	48.15	3.67	6.67
Afterburner	3.20	5.01	3.72	5.80	6.55	11.86
Dryer	5.95	9.33	5.96	9.29	5.88	10.64
Gas cleanup	1.34	2.09	1.05	1.63	0.72	1.30
Heat exchanger	12.66	19.84	13.33	20.78	25.65	46.44
Blower-1	0.43	0.67	0.40	0.63	0.00	0.00
Blower-2	2.51	3.93	2.70	4.20	5.54	10.03
ASU	-	-	0.00	0.01	0.00	0.00
Steam generator	4.41	6.91	3.59	5.61	1.30	2.35
Water pump	0.00	0.00	0.00	0.00	0.00	0.00
Inverter	1.00	1.57	1.07	1.67	2.21	3.99

Table 9: Exergy loss ratio

	Case 1	Case 2	Case 3
y_L [%]	5.28	5.14	5.63

CONCLUSIONS

A model for integrated SOFC and biomass gasification systems is developed. For this purpose, a transient heat transfer model for SOFC which was developed by the authors in a previous study and thermodynamic models for the rest of the components are used. The effect of gasification agent on the performance of the system is discussed. This study shows that steam gasification yields the highest electrical efficiency, power-to-heat ratio and exergetic efficiency, but the lowest fuel utilization efficiency. For the given data, it is found that electrical, fuel utilization and exergetic efficiencies for case-3 are 41.8%, 50.8% and 39.1%, respectively, and the power-to-heat ratio is 4.649. Exergy analysis shows that the largest portion of exergy is destructed in the gasifier cases 1 and 2; whereas exergy destruction is the highest at the heat exchanger used for heating the air entering the SOFC for case-3.

NOMENCLATURE

C	weight percentage of carbon in biomass
ex	specific molar exergy, J/mole
$\dot{E}x$	exergy flow rate, W
FUE	fuel utilization ratio
$\bar{h}$	specific molar enthalpy, J/mole
H	weight percentage of hydrogen in biomass
$\dot{H}$	enthalpy flow rate, W
K	chemical equilibrium constant
LHV	lower heating value, J/mole
m	molar ratio of water to dry biomass
M	molecular weight, g/mole
n	number
$\dot{n}$	molar flow rate, mole/s
N	weight percentage of nitrogen in biomass
O	weight percentage of oxygen in biomass
P	pressure, bar
PHR	power to heat ratio
q	specific molar heat, J/mole
$\dot{Q}$	heat rate, W
R	universal gas constant, J/mole-K
T	temperature, K
y	exergetic ratio
w	power output of a single cell, W
$\dot{W}$	power output, W
x	molar concentration

Greek Letters

ρ	density, g/cm^3
η	efficiency
$\Delta\bar{g}$	change in specific molar gibbs free energy, J/mole
ν	specific volume, cm^3/g
ε	exergetic efficiency
β	exergetic correlation constant
λ	molar ratio of steam entering the gasifier to the drybiomass
μ	chemical potential, J/mole

Subscripts

cps	*cell per stack*
D	*destruction*
el	*electrical*
F	*fuel*
L	*loss*
m	methanation
o	standard
P	product
req	required
tot	total
wgs	water gas shift reaction

Superscripts

CH	chemical
PH	physical

REFERENCES

Achenbach, E. 1996. *SOFC Stack Modelling*. Final Report of Activity A2, Annex II: Modelling and Evaluation of Advanced Solid Oxide Fuel Cells, International Energy Agency Programme on R, D&D on Advanced Fuel Cells, Juelich, Germany.

Athanasiou, C., Coutelieris, F., Vakouftsi, E., Skoulou, V., Antonakou, E., Marnellos, G., and A. Zabaniotou. 2007. From biomass to electricity through integrated gasification/SOFC system-optimization and energy balance. *International Journal of Hydrogen Energy* 32:337-342.

Bejan, A., Tsatsaronis G., and M. Moran. 1996. *Thermal design and optimization*. John Wiley and Sons Inc. U.S.A.

Colpan, C.O., Dincer, I, and F. Hamdullahpur. 2008. Transient modeling of direct internal reforming planar solid oxide fuel cells. *Proceedings of the ASME 2008 Summer Heat Transfer Conference*. August 10-14, 2008, Miami, Florida, USA.

Cordiner, S., Feola, M., Mulone,V. and F. Romanelli. 2007. Analysis of a SOFC energy generation system fuelled with biomass reformate. *Applied Thermal Engineering* 27:738-747.

Dincer, I. and M.A. Rosen. 2007. *Exergy: Energy, Environment and Sustainable Development*. Elsevier. UK.

Goldemberg, J., and T.B. Johansson (editors). 2004. *World Energy Assessment: Overview 2004 Update*. United Nations Development Programme. New York, U.S.A.

International Energy Agency. 2007. *Renewables in Global Energy Supply*. An IEA Fact Sheet. France.

Omosun, A.O., Bauen, A., Brandon, N.P., Adjiman, C.S., and D. Hart. 2004. *Modelling system efficiencies and costs of two biomass-fuelled SOFC systems*. Journal of Power Sources. 131:96-106

Panopoulos, K.D., Fryda, L.E., Karl, J., Poulou, S., and E. Kakaras. 2006[1]. *High temperature solid oxide fuel cell integrated with novel allothermal biomass gasification Part I: Modelling and feasibility study*. Journal of Power Sources. 159:570-585

Panopoulos, K.D., Fryda, L.E., Karl, J., Poulou, S., and E. Kakaras. 2006[2]. *High temperature solid oxide fuel cell integrated with novel allothermal biomass gasification Part II: Exergy analysis*. Journal of Power Sources. 159:586-594

Schmersahl, R. and V. Scholz. 2005. *Testing a PEM fuel cell system with biogas fuel*. Agricultural Engineering International: the CIGR Ejournal. 7. Manuscript EE 05 002.

Szargut, J., Morris, D.R., and F.R. Steward. 1988. *Exergy analysis of thermal, chemical, and metallurgical processes*. Hemisphere. New York. pp.297-309

Szargut, J. 2005. *Exergy method-Technical and ecological applications*. WIT Press. Boston.

Xenergy. 2002. *Toward a Renewable Power Supply: The Use of Bio-based Fuels in Stationary Fuel Cells*.